



A Journal of the Gesellschaft Deutscher Chemiker

Angewandte Chemie

GDCh

International Edition

www.angewandte.org

Accepted Article

Title: Modulating Guest Uptake in Core-Shell MOFs with Visible Light

Authors: Dragos Mutruc, Alexis Goulet-Hanssens, Sam Fairman, Sebastian Wahl, Annett Zimathies, Christopher Knie, and Stefan Hecht

This manuscript has been accepted after peer review and appears as an Accepted Article online prior to editing, proofing, and formal publication of the final Version of Record (VoR). This work is currently citable by using the Digital Object Identifier (DOI) given below. The VoR will be published online in Early View as soon as possible and may be different to this Accepted Article as a result of editing. Readers should obtain the VoR from the journal website shown below when it is published to ensure accuracy of information. The authors are responsible for the content of this Accepted Article.

To be cited as: *Angew. Chem. Int. Ed.* 10.1002/anie.201906606
Angew. Chem. 10.1002/ange.201906606

Link to VoR: <http://dx.doi.org/10.1002/anie.201906606>
<http://dx.doi.org/10.1002/ange.201906606>

Modulating Guest Uptake in Core-Shell MOFs with Visible Light

Dragos Mutruc, Alexis Goulet-Hanssens, Sam Fairman,[†] Sebastian Wahl, Annett Zimathies,[‡] Christopher Knie, and Stefan Hecht*

Abstract: A two-component core-shell UiO-68 type MOF with a non-functionalized interior for efficient guest uptake and storage and a thin light-responsive outer shell was prepared by initial solvothermal MOF synthesis followed by solvent assisted linker exchange. The bulky shell linker features two tetra-*ortho*-fluorinated azobenzene moieties to exploit their advantageous photoisomerization properties. The obtained perfect octahedral single MOF crystals can be switched repeatedly and with an unprecedented efficiency between *E*- and *Z*-rich states using visible light only. Due to the high photoswitch density per pore of the shell layer, its steric demand and thus molecular uptake (and release) can be conveniently modulated upon green and blue light irradiation. Therefore, the “smart” shell acts as a light-controlled kinetic barrier or “gate” for the diffusion of cargo molecules in and out of the MOF crystals.

Materials that are able to adapt their structure in response to external stimuli, such as temperature, pH, mechanical stress as well as electric, magnetic and electromagnetic fields, enjoy increasing attention for various applications.¹ Light is arguably the most attractive among these stimuli as it is tunable in wavelength and intensity, provides unparalleled spatio-temporal resolution, and it can be applied in a remote and non-invasive fashion. Metal-organic frameworks (MOFs) are a promising class of crystalline, porous solids with exceptionally high accessible internal surface areas, consisting of metal nodes or clusters connected with organic linker molecules.² Recent examples have shown that incorporating molecular switches is a viable strategy to obtain light-responsive MOFs.³ The thus required light-induced reversible changes of the pore size or polarity render azobenzenes⁴ an optimal photoswitch class to be used. Most of these photoswitchable MOFs involve the modulation of uptake and separation of gases, using the polarity change upon photoisomerization.⁵ There are only few examples for the release of larger guest molecules into solution, however, exploiting the light-induced mechanical motion of azobenzenes rather than a change in the pore size.⁶ One of the severe drawbacks of these systems is the necessity to use UV light to operate the azobenzene photoswitches. On the one hand, high energy UV light can induce photodegradation of the material, and on the other hand, its penetration into the material is limited, resulting in rather low isomerization efficiencies in the MOF crystals and thus limited photomodulation of their properties. One solution to this problem is the use of *ortho*-fluorinated azobenzenes, which can be switched in both directions using visible light only.⁷ Although there are a few examples that involve the use of bis-*ortho*-fluorinated azobenzenes,⁸ the full potential of tetra-*ortho*-fluoroazobenzenes⁷ was not exploited. Another approach makes use of thin-film surface-mounted metal-organic framework (SURMOF) structures, in which the photoswitchable azobenzene component is only present in the

outer layers.⁹ The latter serve as a light-controlled valve to gate the access to the underlying non-functionalized storage compartment. Although these photoswitchable SURMOFs can be used as membranes for the light-controlled modulation of uptake and separation of gas mixtures, they are limited in scope.

Here, we report on the synthesis and characterization of a two-component core-shell MOF with a large and porous interior for guest storage covered by a thin photoswitchable outer shell, which functions as a light-controlled barrier for uptake and release of guest molecules. Our system is based on well-defined octahedral UiO-68¹⁰ type MOF crystals with a photoresponsive outer shell, introduced by solvent assisted linker exchange (SALE).¹¹ Our linker design was motivated by the concept of a light-responsive MOF with large pores gated by large photoswitchable “doors”, resulting in a *p*-terphenyl-dicarboxylic acid containing two tetra-*ortho*-fluorinated azobenzenes (**L^{azo}**, Figure 1), known to be among the best performing azobenzene switches.⁷ We intentionally doubled their density since Heinke and co-workers could show that the photomodulation of guest uptake depends mostly on the number of azobenzenes per pore volume.¹²

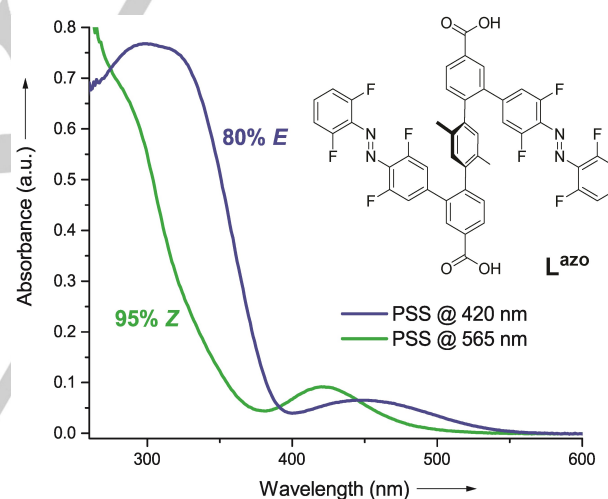


Figure 1. Chemical structure of bisazobenzene-terphenyl linker **L^{azo}** and UV/vis spectra of the photostationary state (PSS) mixtures upon irradiation with green ($\lambda_{\text{irr}} = 565$ nm) and blue ($\lambda_{\text{irr}} = 420$ nm) light (21 μM in DMSO at 25 °C). PSS composition according to UPLC-MS analysis (see Figure S3).

Photoswitchable linker **L^{azo}** was prepared using a 13-step convergent synthesis in an overall yield of 4% (see Supporting Information for details of the synthesis and compound characterization). Initially, the photoisomerization behavior was investigated in solution (Figure 1). Irradiation with green light ($\lambda_{\text{irr}} = 565$ nm) for 20 min results in nearly quantitative *E*→*Z* photoisomerization. According to chromatographic analysis (see Figure S3c) the three isomers, i.e. *Z,Z*, *Z,E*, and *E,E*, are present in a 90.4 : 9.2 : 0.4 ratio, giving rise to the formation of an overall 95% *Z*-configured azobenzene moieties in the photostationary state (PSS). Backward *Z*→*E* photoisomerization is induced upon irradiation with blue light ($\lambda_{\text{irr}} = 420$ nm) and after 10 min a PSS with 80% *E*-configured azobenzene content is reached (*E,E* : *Z,E* : *E,E* = 63.5 : 33.0 : 3.5). Importantly, alternating irradiation with green and blue light does not lead to any noticeable fatigue after eight switching cycles (see Figure S3d). The thermal half-life of the individual *Z*-azobenzene subunits was found to be around 46 d at room temperature (see Figure S5 and S6). Due to the twisted terphenyl core, both azobenzene subunits are electronically decoupled as reflected

[*] D. Mutruc, A. Goulet-Hanssens, S. Wahl, C. Knie, Prof. S. Hecht
Department of Chemistry & IRIS Adlershof
Humboldt-Universität zu Berlin
Brook-Taylor Str. 2, 12489 Berlin, Germany.
E-mail: sh@chemie.hu-berlin.de

[†] S. Fairman
Department of Physics
Humboldt-Universität zu Berlin
Newtonstr. 15, 12489 Berlin, Germany.

[‡] A. Zimathies
Federal Institute for Materials Research and Testing (BAM)
12200 Berlin, Germany.
Supporting information for this article is given via a link at the end of the document.

by the UV/vis absorption spectra showing clean isosbestic points.¹³ This is furthermore supported by cyclic voltammetry, differential pulse polarography, and coulometric analysis (see Figure S7), showing two independent one-electron reduction processes. Importantly, these findings strongly suggest that photoswitching of one azobenzene subunit is independent of the other azobenzene's configuration.

In addition to offering an exceptionally high internal surface area, the zirconium based UiO-68 type MOF was chosen for its known robustness and stability towards water, acids, and heat.¹⁰ Core-MOF I was prepared from the C₂ symmetrical linker L^{core} having terminal salicylic acid functionalities as well as internal methyl groups, mimicking the twisted structure of L^{azo} (Figure 2a, see Supporting Information for synthesis and characterization). Using standard UiO-68 synthetic conditions with benzoic acid (50 equiv.) acting as the modulator¹⁴ resulted in highly crystalline MOF particles of perfect octahedral shape (see Supporting Information for MOF synthesis and Figure S8 for Scanning Electron Microscopy (SEM) and Transmission Electron Microscopy (TEM) images). Gas sorption analysis of activated samples shows a high calculated Brunauer-Emmett-Teller (BET) surface area of 2500 m²/g (see Figure S9) and a narrow pore size distribution reflected in a single peak at around 1.05 nm (see Figure S10), rendering Core-MOF I an ideal storage compartment for our desired core-shell system. The shell was introduced through solvent-assisted linker exchange (SALE, Figure 2a) by stirring Core-MOF I in a solution of linker L^{azo} in 1,4-dioxane at 80 °C for several days. Depending on the reaction time, the shell thickness as determined by digestion and

chromatographic analysis (see Supporting Information for analytic details) could be modulated (see Figure S11). However, the extreme bulkiness of linker L^{azo} led to very slow exchange and a shell of only 8.9% (referring to the molar ratio of L^{azo} to the total amount of linkers, i.e. L^{azo} + L^{core}) could be built up after 21 days, most likely due to hindered diffusion into the MOF pores. Since our goal was to produce a two-component core-shell MOF with a large storage compartment and a light-responsive "gate", a thin shell is highly advantageous. The thus prepared Core-Shell-MOF II was washed excessively until no linker molecules were found in solution. To make sure that no unreacted linker molecules were still trapped as guests inside the porous MOF, we compared the FT-IR spectra of shell linker L^{azo}, Core-MOF I, and Core-Shell-MOF II (see Figure S12). The strong C=O stretching mode at 1680 cm⁻¹ of the carboxylic acid was missing in both, the core and the core-shell MOF, originating from the fact that all linkers are coordinated to the metal clusters as carboxylates. Thermal gravimetric analyses (TGA) of activated samples of I and II show a similar thermal stability until about 370 °C, above which major decomposition occurs (see Figure S13). Despite the rather thin shell, the higher molecular mass of its linker is reflected in the analysis of the relative masses of the ZrO₂ residues remaining after heating to 800 °C, which are larger for I as compared to II.

The powder X-ray diffraction (pXRD) patterns show no change after SALE, meaning that the crystal lattice of the core MOF is fully retained (Figure 2b). SEM and TEM images of Core-Shell-MOF II confirm this as well (Figures 3a,b) and the perfect single crystal octahedra remain unchanged after SALE. Characterization of the MOF crystals by either TEM or SEM demanded careful preparation of the MOF dispersion. The MOF crystals were strongly aggregating due to electrostatic charging, however, adding LiBr to the dispersion resulted in partial breakdown of these aggregates and allowed for successful imaging and analysis of single crystals (Figure 3b). Dynamic light scattering (DLS) analysis at different angles shows an average hydrodynamic radius of 376 nm and a polydispersity index (PDI) of 0.24, indicating a moderate size distribution of II (see Figure S14). To confirm that the shell in II is truly a shell and not distributed randomly throughout the entire crystal, we investigated our MOF samples with energy-dispersive X-ray spectroscopy (EDX). EDX line scans from the center of an octahedral crystal to its apex were performed and the signals for fluorine and zirconium were plotted along this line (Figures 3c,d).

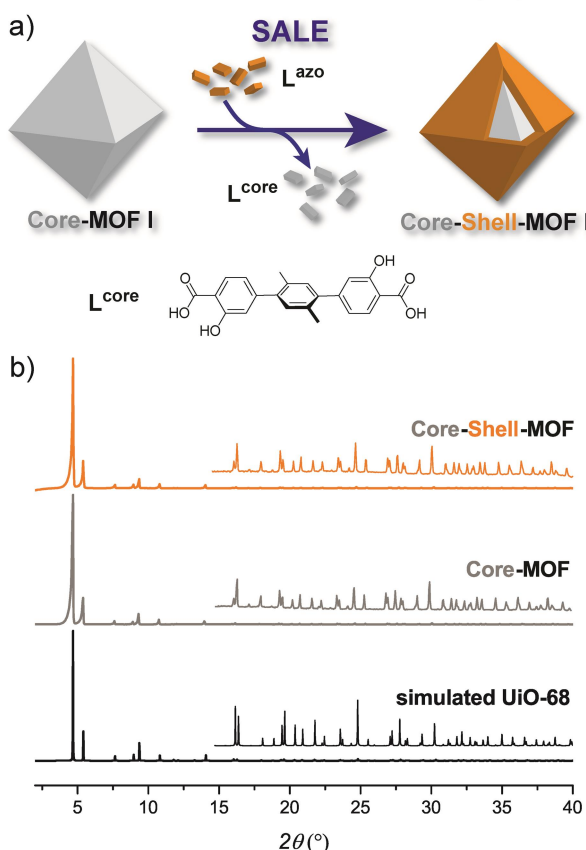


Figure 2. a) Solvent-assisted linker exchange (SALE) on Core-MOF I (grey octahedron) with azobenzene linker L^{azo} affords Core-Shell-MOF II with a thin photoresponsive shell (orange octahedron with grey interior). b) pXRD patterns of Core-MOF I and Core-Shell-MOF II as well as the simulated diffraction pattern for UiO-68 based on its known crystal lattice.¹⁴ In all diffraction patterns, insets show the magnified range from 15 ° to 40 °.

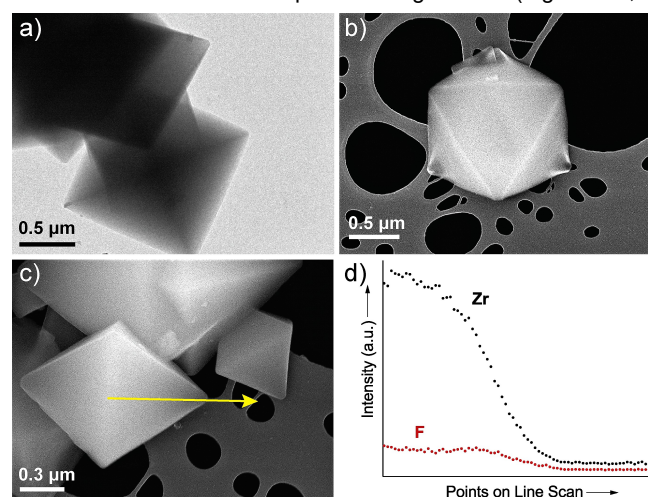


Figure 3. a) TEM and b) SEM images of Core-Shell-MOF II showing perfect octahedral crystals. c) SEM image of Core-Shell-MOF II sample with direction and location of the EDX line scan performed on a single crystal (1000 nm edge length) and d) thus obtained EDX plot showing the distribution of zirconium and fluorine.

The fact that the azobenzene linker contains fluorine and the core linker does not, allowed us to compare the distribution of the shell with regard to the entire MOF crystal as judged by the zirconium signal. While the latter shows the expected bell-type curve from the center of the crystal to the apex due to the constantly decreasing thickness, the fluorine signal plateaus and decreases only at the edge of the crystal. This provides very strong evidence for an outer shell of reasonably uniform thickness and is supported further by corresponding elemental mapping in SEM images (see Figure S15). Additional EDX line scans on crystals of different sizes (650 and 1275 nm edge length) were performed and exhibit the same behavior, showing that the core-shell structure is independent of the size of the particles (see Figures S16 and S17).

The photoisomerization behavior of Core-Shell-MOF II samples with an 8.9% shell was analyzed in the solid state by diffuse reflectance spectroscopy and the resulting data (see Figure S18) transformed to the respective absorption spectra (Figure 4a). Irradiation with either green ($\lambda_{\text{irr}} = 565 \text{ nm}$) or blue light ($\lambda_{\text{irr}} = 420 \text{ nm}$) resulted in a characteristic shift of the $n \rightarrow \pi^*$ absorption band known for *ortho*-fluorinated azobenzenes.⁷ Even after multiple cycles of alternating irradiation no fatigue was observed (Figure 4a, inset). To determine the composition

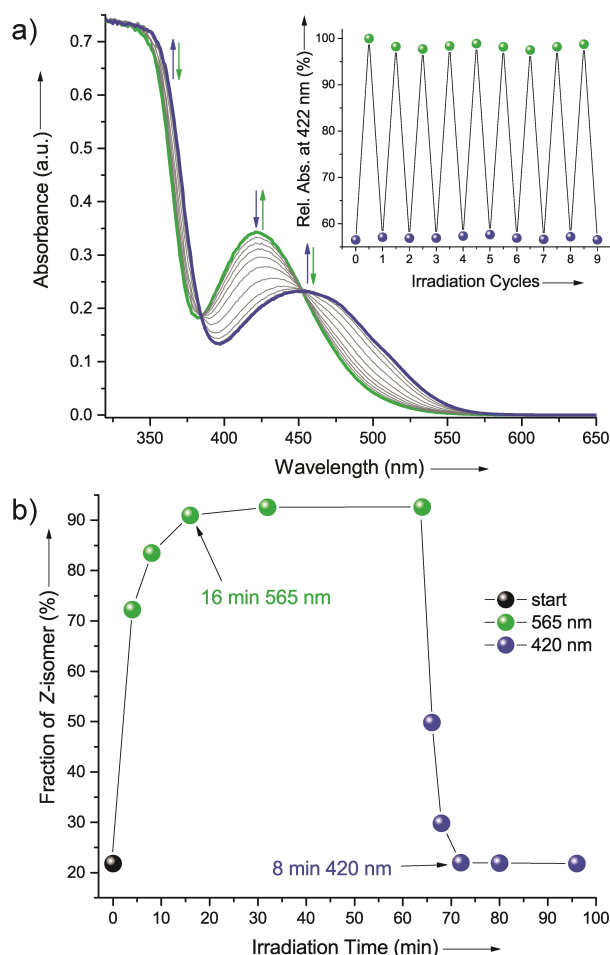


Figure 4. a) Absorption spectra of solid Core-Shell-MOF II samples upon irradiation with green ($\lambda_{\text{irr}} = 565 \text{ nm}$) or blue ($\lambda_{\text{irr}} = 420 \text{ nm}$) light as recorded by diffuse reflectance spectroscopy and converted using the Kubelka-Munk function. The inset shows the relative absorbance at 422 nm ($n \rightarrow \pi^*$ band of the Z-isomer) over several switching cycles. b) Determination of photoconversion by digestion analysis of a Core-Shell-MOF II sample after irradiation with green ($\lambda_{\text{irr}} = 565 \text{ nm}$) or blue ($\lambda_{\text{irr}} = 420 \text{ nm}$) light in solution ($\sim 1.0 \text{ mg MOF}$ in 2 mL of acetonitrile).

of the PSS, samples of II were dispersed in acetonitrile and after irradiation, the MOF particles were digested and analyzed by ultra-performance liquid chromatography coupled to mass spectrometry (UPLC-MS, see Figure S19). According to this digestion analysis, irradiation with green light leads to a PSS after approximately 20 minutes containing 93% Z-isomer, whereas irradiation with blue light gives a PSS after only 8 minutes composed of 78% E-isomer (Figure 4b). This result is quite remarkable since the isomer ratios in the PSSs in the solid MOF samples are practically as high as for the free azobenzene linker L^{azo} in solution. Importantly, pXRD patterns after green and blue light exposure show that the MOF particles retain their crystallinity (see Figure S20), proving the structural integrity of the materials during irradiation cycles.

As a first demonstration of the potential application as a container with a light-responsive shell we performed molecular uptake and release experiments with Core-Shell-MOF II (8.9% shell). MOF crystals were irradiated with green light to facilitate the loading with 1-pyrenecarboxylic acid, then irradiated back to the E-rich sample using blue light, and excessively washed after loading to assure that no guest molecules were adsorbed to the outer surface of the crystals (see Supporting Information for details). Subsequent release experiments were performed in a static setup with the loaded MOF particles located at the bottom of a cuvette, in which the fluorescence signal of the released guest in the overlying ethanol layer was monitored. Indeed, after 5 h the release of the Z-rich loaded sample, obtained after green light irradiation of the solid, was 37% higher as compared to the E-rich loaded sample (see Figure S21). We reason that the observed modest difference in release kinetics is due to the initial infinite concentration gradient leading to rapid diffusion of the guest molecules out of the MOF into the solvent, in both shell configurations. Thus, we explored inherently slower uptake experiments to demonstrate a more pronounced effect of the light-responsive azobenzene shell. In this case, the uptake of the guest was tracked by UV-vis spectroscopy and shows a significant increase of 86% for the Z-rich MOF sample after 78 h (Figure 5). The difference between the E-rich Core-Shell-MOF II and the Core-MOF I is even higher and amounts to 200% after 60 h (see Figure S23). Looking at the early stages of the experiment, we could observe an immediate uptake into the Core-MOF I, whereas the uptake in the Core-Shell-MOF II only begins after several hours and is slower for the E-rich as

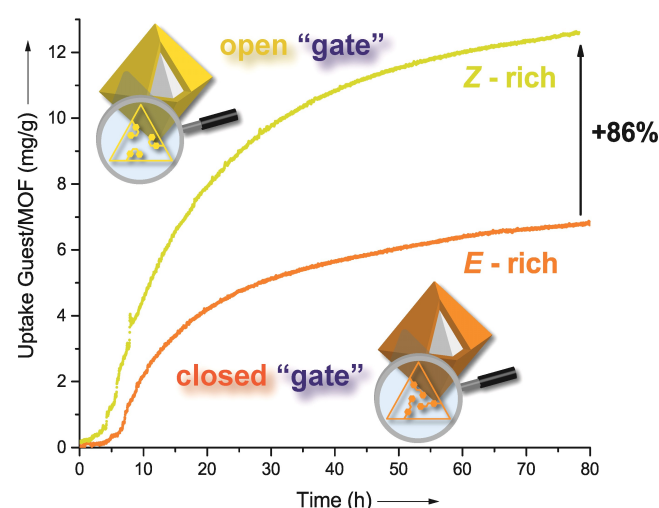


Figure 5. Uptake experiments of 1-pyrenecarboxylic acid by Core-Shell-MOF II for the different photoisomerization states of the shell (E-rich: 78% E-isomer content, Z-rich: 91% Z-isomer content) as monitored by UV/vis spectroscopy. MOF particles were irradiated prior to the measurement (see Supporting Information for details).

compared to the Z-rich shell, demonstrating that the shell is functioning as a kinetic barrier for the diffusion of guests into the pores. A similar, yet less pronounced initial difference was also observed in the release experiments. Uptake experiments with two other guests, methylene blue and 8-hydroxypyrene-1,3,6-trisulfonic acid trisodium salt (HPTS), were also performed and show a similar uptake behavior for the different setups. The uptake of methylene blue is much faster, presumably due to its smaller size as compared to the pyrene derivatives, yet the modulation upon photoisomerizing the shell is less pronounced. The opposite can be observed for the larger HPTS guest (see Figures S24 and S25).

In conclusion we have developed a UiO-68 based two-component core-shell MOF composed of a non-functionalized interior for storage of guest molecules and a light-responsive outer shell acting as a gate for their uptake and release in solution. The MOF crystals obtained by a two-step growth and ligand exchange procedure show a perfectly defined octahedral shape and a narrow size distribution. The shell's bis(tetra-*ortho*-fluoro-azobenzene) terphenyl linker was designed to increase both the azobenzene density and the degree of photoconversion under visible light only. Indeed, the resulting core-shell MOFs possess remarkable photoisomerization properties, reaching PSS compositions nearly as high as for the free linker in solution, highlighting the importance of photoswitch design for crystalline materials. Uptake experiments show a significant difference between both switching, i.e. *E*-rich and *Z*-rich, states, confirming the large steric modulation upon photoisomerization. Our findings demonstrate that the azobenzene-ligand shell is acting as a photoresponsive kinetic barrier for the diffusion in (and out) of the MOF interior. In a next step, we are currently aiming at implementing catalytically active cores to exploit our light-responsive shell as a "selectivity filter" to modulate the access of substrates and thus influence the outcome of the reaction.

Acknowledgements

The authors thank Jana Hildebrandt and Jutta Schwarz for up-scaling the synthesis of linkers L^{azo} and L^{core} , Dr. Matthias Karg for pXRD measurements, Dr. Björn Kobin for TGA, Dr. Lutz Grubert for electrochemistry, and Svante Ihrig for the design of the TOC figure. A.G.-H. is indebted to the Alexander von Humboldt-Foundation and the FQRNT for providing postdoctoral fellowships. Generous support by the Deutsche Forschungsgemeinschaft (Projektnummer 182087777 - SFB 951 and BL 1269 "Visimat"), the Daimler Benz-Foundation (via 32-02/14) as well as the European Research Council (via ERC-2012-StG_308117 "Light4Function") is gratefully acknowledged.

Conflict of Interests

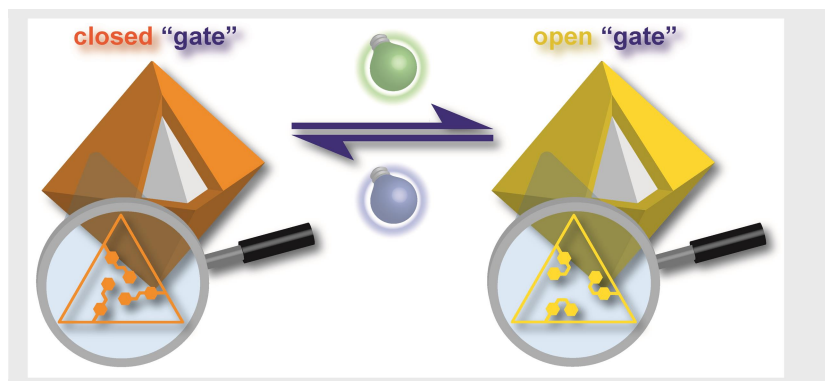
The authors declare no conflict of interest.

Keywords: azobenzene • guest uptake/release • metal-organic frameworks • photochromism • visible light

- [1] a) M. A. C. Stuart, W. T. S. Huck, J. Genzer, M. Müller, C. Ober, M. Stamm, G. B. Sukhorukov, I. Szeifler, V. V. Tsukruk, M. Urban, F. Winnik, S. Zauscher, I. Luzinov, S. Minko, *Nat. Mater.* **2010**, *9*, 101-113; b) R. J. Wojtecki, M. A. Meador, S. J. Rowan, *Nat. Mater.* **2011**, *10*, 14-27; c) E. M. White, J. Yatvin, J. B. Grubbs, J. A. Bilbrey, J. Locklin, *J. Polym. Sci. Part B: Polym. Phys.* **2013**, *51*, 1084-1099; d) M. Wei, Y. Gao, X. Li, M. J. Serpe, *Polym. Chem.* **2017**, *8*, 127-143; e) *Smart Light-Responsive Materials: Azobenzene-Containing Polymers and Liquid Crystals*, (Eds.: Y. Zhao, T. Ikeda), Wiley, Hoboken, **2009**.
- [2] Original work: a) O. M. Yaghi, G. Li, H. Li, *Nature* **1995**, *378*, 703-706. Reviews: b) M. O'Keeffe, M. A. Peskov, S. J. Ramsden, O. M. Yaghi, *Acc. Chem. Res.* **2008**, *41*, 1782-1789; c) G. Férey, *Chem. Soc. Rev.* **2008**, *37*, 191-214; d) S. Horike, S. Shimomura, S. Kitagawa, *Nat. Chem.* **2009**, *1*, 695-704; e) M. O'Keeffe, O. M. Yaghi, *Chem. Rev.* **2012**, *112*, 675-702.
- [3] First examples: a) A. Modrow, D. Zargarani, R. Herges, N. Stock, *Dalton Trans.* **2011**, *40*, 4217-4222; b) A. Modrow, D. Zargarani, R. Herges, N. Stock, *Dalton Trans.* **2012**, *41*, 8690-8696. Reviews: c) S. Castellanos, F. Kapteijn, J. Gascon, *CrystEngComm* **2016**, *18*, 4006-4012; d) A. B. Kanj, K. Müller, L. Heinke, *Macromol. Rapid Commun.* **2018**, *39*, 1700239.
- [4] Reviews: a) H. M. D. Bandara, S. C. Burdette, *Chem. Soc. Rev.* **2012**, *41*, 1809-1825; b) M.-M. Russew, S. Hecht, *Adv. Mater.* **2010**, *22*, 3348-3360.
- [5] a) J. Park, D. Yuan, K. T. Pham, J.-R. Li, A. Yakovenko, H.-C. Zhou, *J. Am. Chem. Soc.* **2012**, *134*, 99-102; b) Z. Wang, S. Grosjean, S. Bräse, L. Heinke, *ChemPhysChem* **2015**, *16*, 3779-3783; c) Z. Wang, A. Knebel, S. Grosjean, D. Wagner, S. Bräse, C. Wöll, J. Caro, L. Heinke, *Nat. Commun.* **2016**, *7*, 13872; d) H. Huang, H. Sato, T. Aida, *J. Am. Chem. Soc.* **2017**, *139*, 8784-8787.
- [6] a) J. Brown, B. L. Henderson, M. D. Kiesz, A. C. Whalley, W. Morris, S. Grunder, H. Deng, H. Furukawa, J. I. Zink, J. F. Stoddart, O. M. Yaghi, *Chem. Sci.* **2013**, *4*, 2858-2864; b) X. Meng, B. Gui, D. Yuan, M. Zeller, C. Wang, *Sci. Adv.* **2016**, *2*, e1600480.
- [7] a) D. Blegler, J. Schwarz, A. M. Brouwer, S. Hecht, *J. Am. Chem. Soc.* **2012**, *134*, 20597-20600; b) C. Knie, M. Utecht, F. Zhao, H. Kulla, S. Kovalenko, A. M. Brouwer, P. Saalfrank, S. Hecht, D. Bléger, *Chem. Eur. J.* **2014**, *20*, 16492-16501.
- [8] a) S. Castellanos, A. Goulet-Hanssens, F. Zhao, A. Dikhtiarenko, A. Pustovarenko, S. Hecht, J. Gascon, F. Kapteijn, D. Blegler, *Chem. Eur. J.* **2016**, *22*, 746-752; b) K. Müller, A. Knebel, F. Zhao, D. Bléger, J. Caro, L. Heinke, *Chem. Eur. J.* **2017**, *23*, 5434-5438.
- [9] L. Heinke, M. Cakici, M. Dommaschk, S. Grosjean, R. Herges, S. Bräse, C. Wöll, *ACS Nano* **2014**, *8*, 1463-1467.
- [10] Original work: J. H. Cavka, S. Jakobsen, U. Olsbye, N. Guillou, C. Lamberti, S. Bordiga and K. P. Lillerud, *J. Am. Chem. Soc.* **2008**, *130*, 42, 13850-13851.
- [11] Review: O. Karagiari, W. Bury, J. E. Mondloch, J. T. Hupp, O. K. Farha, *Angew. Chem. Int. Ed.* **2014**, *53*, 4530-4540.
- [12] Z. Wang, K. Müller, M. Valášek, S. Grosjean, S. Bräse, C. Wöll, M. Mayor, L. Heinke, *J. Phys. Chem. C* **2018**, *122*, 19044-19050.
- [13] M. V. Peters, PhD thesis, Humboldt-Universität zu Berlin, **2008**.
- [14] A. Schaate, P. Roy, A. Godt, J. Lippe, F. Waltz, M. Wiebcke, P. Behrens, *Chem. Eur. J.* **2011**, *17*, 6643-6651.

Entry for the Table of Contents

COMMUNICATION



*Dragos Mutruc, Alexis Goulet-Hanssens, Sam Fairman, Sebastian Wahl, Annett Zimathies, Christopher Knie, and Stefan Hecht**

Page No. – Page No.

Modulating Guest Uptake in Core-Shell MOFs with Visible Light

Light opens and closes the doors to an inner porous storage compartment of azobenzene-containing core-shell MOFs.